Microscopy and Microanalysis of Magmatic and Metamorphic Minerals – Part 1: Cordierite

Robert Sturm
Brunnleitenweg 41, A-5061 Elsbethen, Salzburg/Austria
Robert.Sturm@sbg.ac.at

Introduction

Cordierite represents an orthorhombic (Mg,Fe)Al-silicate (Table 1) that is observed in a wide range of natural occurrences. As outlined in numerous mineralogical overviews published during the past decades[1,2], cordierite mainly crystallizes in thermally metamorphosed rocks, particularly in those derived from argillaceous sediments. Additionally, the mineral can be a major constituent of parageneses formed under high-grade regional metamorphism and therefore occurs in respective schists, gneisses and granulites. The metamorphic formation of cordierite is generally restricted to conditions of deficient or low shearing stress producing only moderate lithological pressures.[3] With rising pressure due to transpression cordierite often breaks down to enstatite and sillimanite or, at higher temperature, to sapphirine and quartz (see also Fig. 5).[2,4] Besides its crystallization in metamorphic rocks, cordierite is also found in specific igneous rocks like peraluminous granites and related high-grade anatectic terrains. Here, the mineral is considered as a product of subsolidus metamorphic reactions, a product of peritectic reactions at the granite source or a derivate of argillaceous material contaminating the granitic magma.[1,5] Among some authors cordierite is also considered as a cotectic magmatic mineral or a mineral phase formed by metasomatism which directly followed the process of granitization.[6,7] Cordierite of gem quality often occurs in granite pegmatites, where it usually crystallizes from uncontaminated pegmatitic liquids. A previous crystallization from residual magmas enriched with Al-silicates is also discussed. Concerning its physical properties being essential for macroscopic and light-microscopic identification, cordierite exhibits some similarities to other minerals, especially to quartz and feldspar (Table 1). In the contribution presented here, cordierite and its specific microscopic/microchemical characteristics are introduced to microscopists with enhanced mineralogical interest. The detailed description of the mineral is conducted using respective samples from an ultramylonite (*i.e.* a fine-grained rock formed by a ductile shearing process) exposed at the South-western margin of the Bohemian Massif in Austria (Fig. 1, 2).

Cordierite - Chemical composition

$(Mg,Fe)_2Al_3[AlSi_5O_{18}]$

Cordierite - Physical properties

Crystal habit	Pseudo-hexagonal prismatic twins, as embedded grains, massive
Color	Blue, violet, yellow-brown; transparent to translucent
Crystal system	Orthorhombic 2/m 2/m 2/m
Cleavage	{010} poor cleavage
Fracture	Conchoidal, uneven
Mohs scale hardness	7 - 7.5
Refractive index	α = 1.522 - 1.558, β = 1.524 - 1.574, γ = 1.527 - 1.578; index increases with Fe content
Optical properties	Usually optical (-), somtimes (+); 2V = 0-90°
Pleochroism	Strong,dichroic: brown-yellow, light and dark blue
Streak	White
Specific gravity	2.57 - 2.66

Table 1. *Overview of the chemical composition and physical properties of cordierite.*

Material and methods

One part of the samples taken from the ultramylonite was used for the production of oriented thin sections, serving for light-microscopy. This was conducted on a petrographic microscope (ZEISS), appropriately equipped for dark-field microscopy. In addition, polished thin sections for micro-chemical analysis and

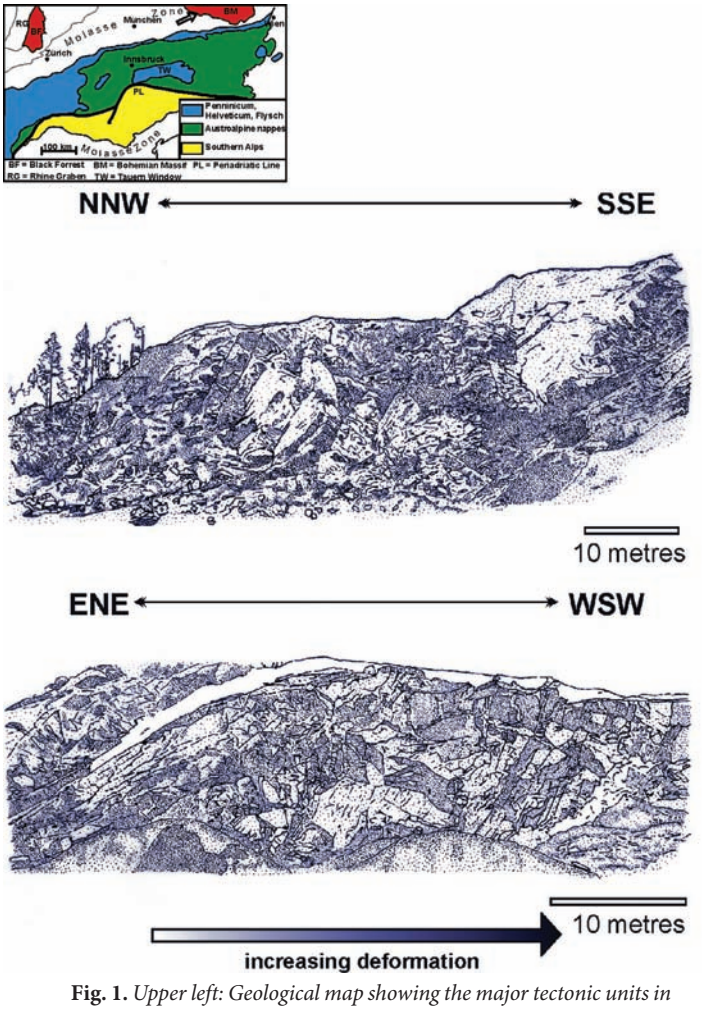

Fig. 1. *Upper left: Geological map showing the major tectonic units in Central Europe and the geographic position of the rocks analyzed in this study; draft exhibiting the quarry, from which cordierite-bearing rocks were sampled.*

DiATOME Diamond Knives

Development, Manufacturing, and Customer Service since 1970

What have we achieved in this period?

ultra 45°
the first diamond knife with an absolutely score-free, hydrophilic cutting edge.

semi
the first diamond knife for alternating sectioning ultrathin/semithin.

cryo
the diamond knife for sectioning at low temperature.

histo
the first diamond knife for semithin sections for light microscopy.

ultra 35°
the diamond knife for optimized sectioning results in almost all applications.

cryo-P
a cryo knife with a patented platform for section pick up.

cryo immuno
the optimized cryo diamond knife for the Tokuyasu technique.

ultra sonic
the oscillating diamond knife for room temperature sectioning.

cryotrim
45 and 25 optimizing trimming with diamond blades.

ultra AFM & cryo AFM
the first diamond knives for AFM at room and low temperatures.

cryo 25°
for sectioning frozen hydrated specimens.

STATIC LINE II
the ionizer for eliminating electrostatic charging in ultramicrotomy.

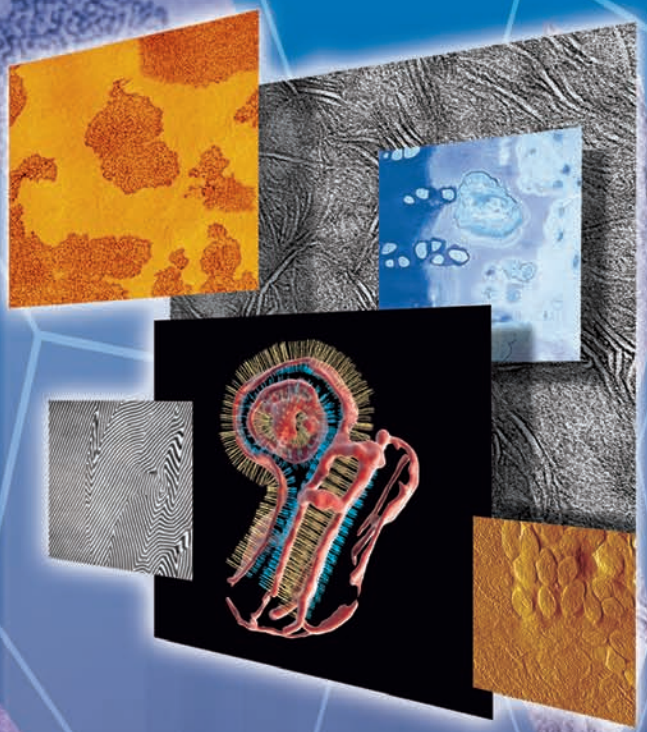

What services can we offer you?

- Technical assistance in all fields of ultramicrotomy.
- Free sectioning tests for all types of samples.
- Make use of our many years of experience in perfecting our knives.
- Custom knives, tools, and boats.
- Special purchase programs.
- Workshops and training.

DiATOME

for all your sectioning requirements

For more information, please call or write us today, or visit us online at:

www.diatomeknives.com

P.O. Box 410 • 1560 Industry Rd.
Hatfield, Pa 19440
(215) 412-8390 • Toll Free: 1-(800) 523-5874
Fax: (215) 412-8450 or 8452
email: sgkcck@aol.com • stacie@ems-secure.com

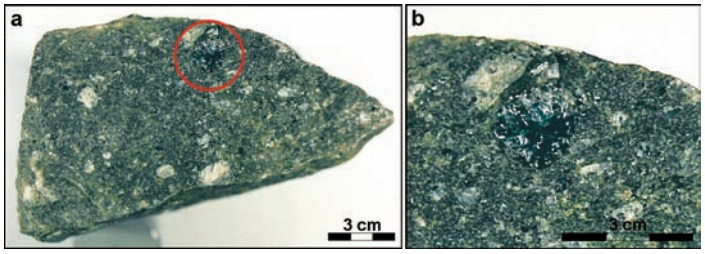

Fig. 2. *Sample of the cordierite-bearing ultramylonite (a) containing a blue cordierite crystal characterized by remarkable size (b).*

back-scattered electron imaging (BSEI) were produced. These procedures were carried out on a JEOL JXA-8600 microprobe at the institute of Geology, University of Salzburg. Operating parameters were set as follows: 30 nA beam current, 15 kV accelerating voltage, 10 s counting time for each element except Ti and Na (30 s), and a constant beam diameter of 1 µm. Natural and synthetic silicates and oxides served as standards for the main element analysis.[8] Correction of the raw analyses was done by the application of an internal ZAF-4 procedure. The element analyses produced experience an average error not exceeding 0.1 wt.%. For Na_2O the detection limit is 0.050 wt.% employing operating parameters as detailed above. Back-scattered electron imaging of unaffected as well as partly and fully decomposed cordierites was carried out by turning up the beam current from 30 nA to 40 nA in order to increase the contrast for photography.

Cordierite from the Bohemian Massif

The ultramylonite as well as its surrounding lithology can be assigned to the Southwestern margin of the Bohemian Massif (Fig. 1). This Variscan massif is mainly located within the Central-European Moldanubian zone[9], characterized by widespread high-temperature/low-pressure metamorphism, partial melting processes and extensive plutonism. The geology of the study area is marked by Variscan migmatites and gneisses of the so-called Monotonous series that have been intruded by post-Variscan granite bodies. During the Tertiary, NW-SE tending strike-slip faults (Pfahl and Danube fault) with variable shear sense were formed and divided the lithology into three main granitic bodies.[10] The rock of the present study was produced in a local dextral shear zone that can be interpreted as a side branch of the Pfahl fault. The quarry, in which the cordierite-bearing ultramylonite is found (Fig. 1: arrow in the map) consists of two orthogonal walls, whereby on the WSW-ENE-tending wall metamorphic rocks with increasing grades of deformation are exposed.

When analyzed macroscopically, the ultramylonite of the ductile shear zone contains cordierite crystals ranging from 0.3 to 20 mm in size (Fig. 2a). Large cordierites that are not, or only slightly, affected by pinitization (*i.e.* decomposition into chlorite and muscovite, see below) are characterized by a medium-to dark-blue colour (Fig. 2b). With progressing decomposition of the mineral, its colour changes continuously to bluish-green.

Microscopy and micro-analysis of cordierite crystals

The ultramylonite displays a mineral assemblage containing the mineral phases K-feldspar + quartz + plagioclase + cordierite + biotite + muscovite + sillimanite (fibrolite) ± garnet ± chlorite ± ilmenite. Under the light-microscope the investigated samples show a matrix formed by very fine-grained quartz and biotite. Both minerals are recrystallized in high amounts (Fig. 3) and can be accumulated to specific aggregates or layers. Biotite is often accompanied by fibrolitic sillimanite and muscovite. The porphyroclasts and -blasts of the rock are mainly represented by feldspar

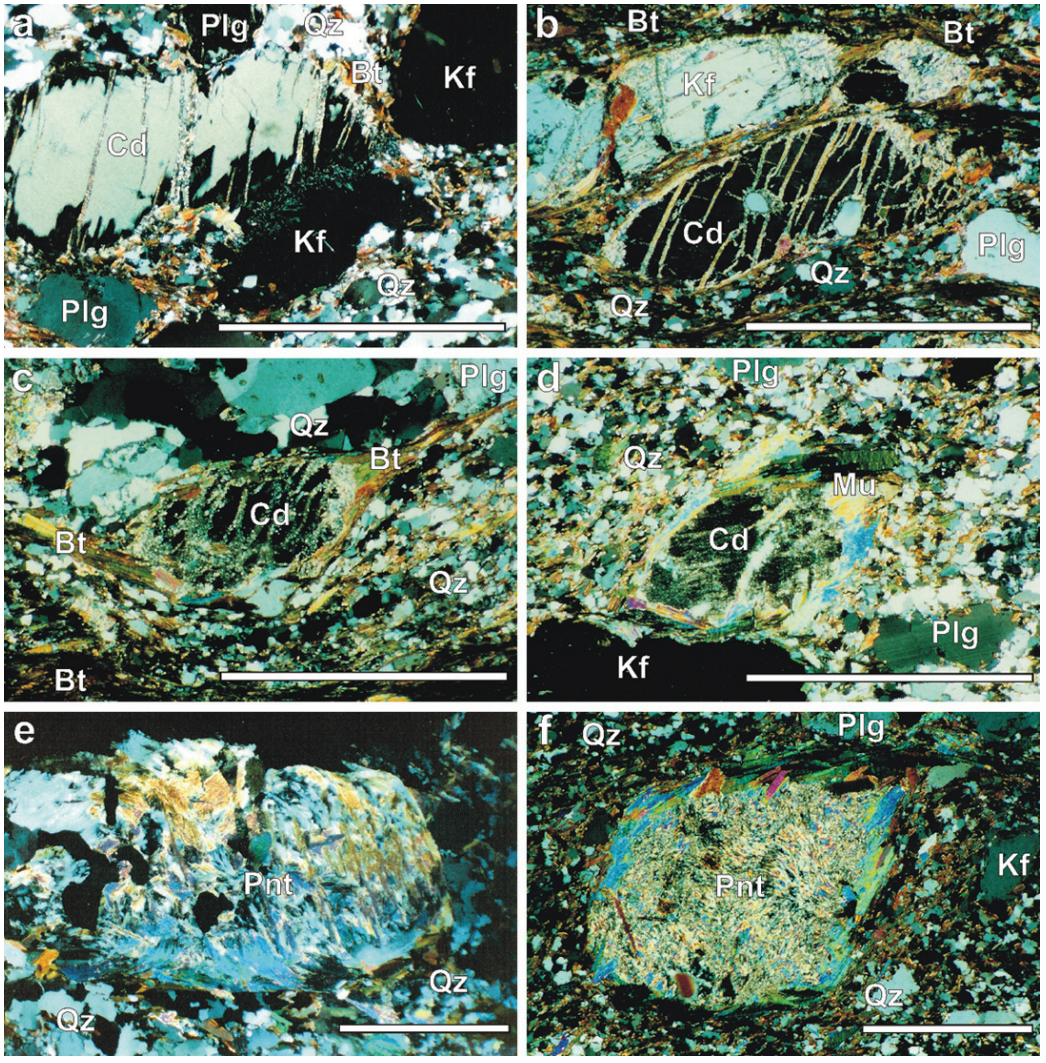

Fig. 3. *Microphotographs of the mineral assemblage, which the ultramylonite is mainly composed of. Unaffected cordierite (Cd) may be identified due to its typical cracks and dark corona (a). During uplift of the rock, cordierite is marked by a continuous decomposition, finally resulting in pinite (Pnt; b-f). Further abbreviations: Bt…biotite, Kf…K-feldspar, Mu…muscovite, Plg…plagioclase, Qz…quartz. Bars represent 1 mm, respectively.*

COLLEGE OF MICROSCOPY

Learn from experience... learn from the experts.

2009 COURSE SCHEDULE

Winter/Spring

Learn from McCrone scientists—

The College of Microscopy is a specialized learning center providing microscopy and spectroscopy education, and is dedicated to quality hands-on teaching of microanalytical principles, techniques, and applications.

Polarized Light Microscopy

COM100
Modern Polarized Light & Chemical Microscopy
May 4-8, 2009

Electron Microscopy

COM200
Scanning Electron Microscopy
March 16-20, 2009

COM210
Advanced Scanning Electron Microscope Based Tools for Microanalysis
February 9-13, 2009

COM250
Transmission Electron Microscopy
March 24-26, 2009

Sample Preparation

COM310
Sample Preparation: Pharmaceutical & Medical Devices
May 18-19, 2009

COM312
Sample Preparation: Forensics & Trace Evidence
June 11-12, 2009

Biological/Medical

COM700
Body Fluid Identification & Microscopical Methods of Sperm Detection for Forensic DNA/Serology/Biology
April 28-30, 2009

Cultural Preservation and Conservation Studies

COM801
Laboratory Safety
June 5, 2009

COM870
Spot Testing for Materials Characterization
May 4-8, 2009

Special Applications

COM400
Microscopical Examination of Forensic Trace Evidence (Part 1)
June 15-19, 2009

COM401
Hair Comparisons & Identification
April 20-24, 2009

COM402
Fiber Identification
April 13-17, 2009

COM410
Microscopical Identification of Pharmaceutical Materials & Contaminants
May 11-15, 2009

COM415
USP {788} Particulate Matter in Injections
May 21, 2009

COM425
Introduction to the Microscopical Identification of Conservation Materials
June 8-12, 2009

COM430
Microscopical Identification of White-Powder Unknowns
February 23-27, 2009

COM450
Freeze-Dry Microscopy
May 5-7, 2009

Imaging/Software

COM520
PAX-it Image Database & Image Analysis Workshop
February 19-20, 2009

Spectroscopy

COM600
Infrared Microscopy
March 24-26, 2009

Educational Outreach

COM900
Microscopy Workshop for Middle & High School Science Teachers
June 22-26, 2009

COM902
Forensic Workshop for Middle & High School Science Teachers
July 13-17, 2009

AUTHORIZED IACET PROVIDER

***Register today*—www.collegeofmicroscopy.com** *College of Microscopy, 850 Pasquinelli Drive, Westmont, IL 60559,* **630-887-7100**

Sample	95/01a			95/01b			95/01c		95/01d	
No.	1.	2.	3.	4.	5.	6.	7.	8.	9.	10.
SiO_2	47.58	47.86	47.90	48.06	47.77	48.05	47.84	47.83	47.96	47.51
Al_2O_3	32.69	32.54	32.55	32.76	32.67	32.66	32.94	32.71	32.52	32.86
FeO	8.85	8.99	8.89	9.31	9.17	9.41	9.54	9.86	9.68	9.22
MgO	6.75	7.13	7.33	6.92	6.96	7.05	6.78	6.45	6.82	6.55
MnO	0.74	0.55	0.41	0.39	0.41	0.40	0.52	0.48	0.45	0.62
CaO	0.03	0.03	-----	0.09	0.03	-----	0.02	0.03	0.05	0.04
K_2O	0.01	0.01	-----	0.02	-----	-----	-----	-----	-----	-----
Na_2O	0.42	0.47	0.45	0.51	0.49	0.50	0.52	0.53	0.57	0.54
Total	97.07	97.58	97.53	98.07	97.50	98.07	98.16	97.89	98.05	97.34
Si	4.994	4.998	4.998	4.998	4.993	4.998	4.979	4.997	5.000	4.981
Al^{T1}	1.006	1.002	1.002	1.002	1.007	1.002	1.021	1.003	1.000	1.019
Al^{T2}	3.069	3.034	3.032	3.044	3.049	3.032	3.049	3.055	3.026	3.073
Fe	0.777	0.785	0.776	0.810	0.802	0.819	0.830	0.861	0.844	0.808
Mg	1.056	1.110	1.140	1.073	1.085	1.093	1.052	1.005	1.066	1.024
Mn	0.066	0.049	0.037	0.034	0.036	0.036	0.046	0.042	0.040	0.055
Ca	0.003	0.003	-----	0.011	0.004	-----	0.002	0.003	0.006	0.004
K	0.001	0.001	-----	0.003	-----	-----	-----	-----	-----	-----
Na	0.085	0.095	0.091	0.103	0.099	0.101	0.105	0.108	0.114	0.109
Total	11.058	11.078	11.076	11.014	11.074	11.081	11.085	11.074	11.090	11.073

Table 2. *Chemical composition of cordierite from the ultramylonite discussed in this study. All together, four rock samples were subject to a micro-chemical analysis using the electron microprobe.*

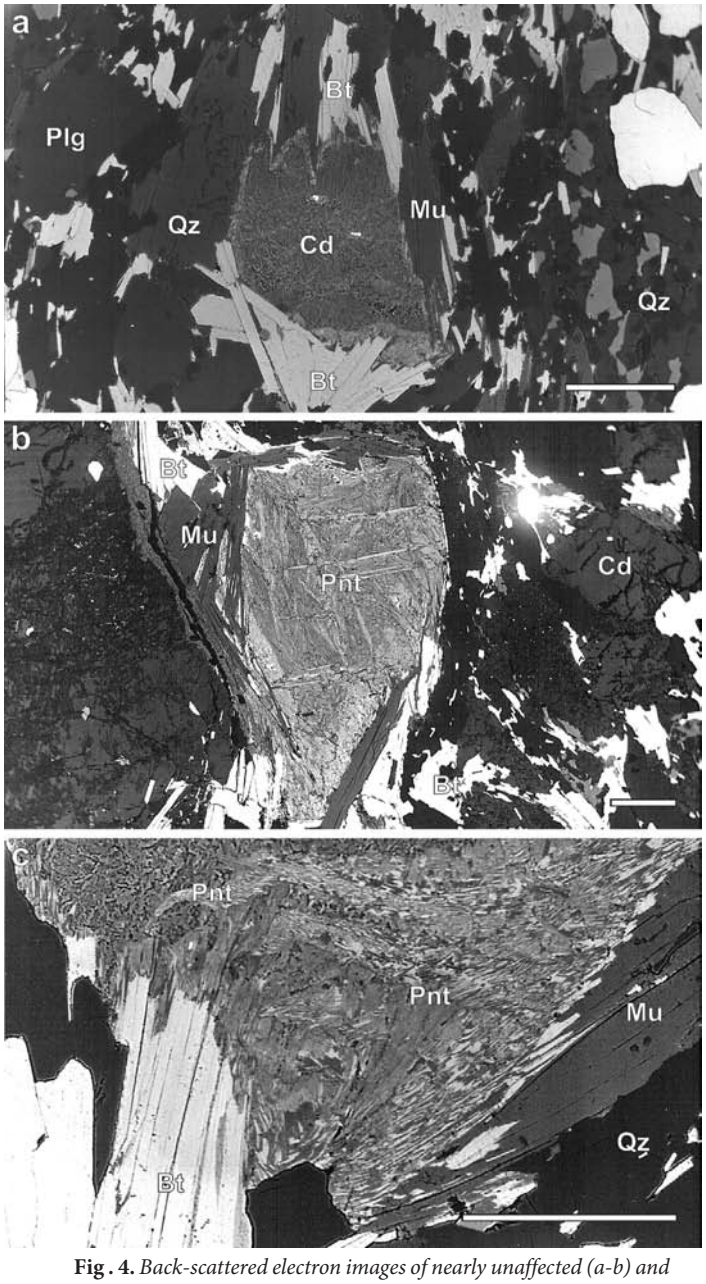

Fig . 4. *Back-scattered electron images of nearly unaffected (a-b) and pinitized cordierites (b-c). For abbreviations see Fig. 3. Bars represent 100 µm, respectively.*

relics and cordierite and partly show a significant rotation parallel to the deformation plane (*e.g.* Fig. 3b).

Under the light-microscope, cordierite crystals appear as isometric to slightly elongated grains surrounded by a fine matrix of quartz, biotite, mica, and sillimanite. Those grains not affected by pinitization (see below), are easily identifiable due to dark cracks and coronas (e.g. Fig. 3a) as well as their typical pleochroism. While ca. 30 % of the grains are free from inclusion phases, the remaining 70 % contain quartz, relictic biotite, sillimanite, and garnet.

Microprobe analyses of cordierite crystals underline that the mineral is characterized by a rather homogeneous chemistry (Table 2). In contrast to the ideal structural formula of cordierite (Table 1), a slight deficiency in Si (< 5.0 p.f.u.) and excess in Al (> 4.0 p.f.u.) can be recognized. The sum of both tetrahedral cations varies between 9.030 and 9.080 and therefore deviates from the ideal value of 9.00 by 0.33 to 0.88 %. The replacement of octahedral Mg by Fe^{2+} and Mn is documented by a Mg/(Mg + Fe^{2+} + Mn) ratio ranging from 0.543 to 0.584. These values confirm a predominance of Mg in the octahedral sites. MnO plays a minor role in the major-element composition, reaching a maximum value of

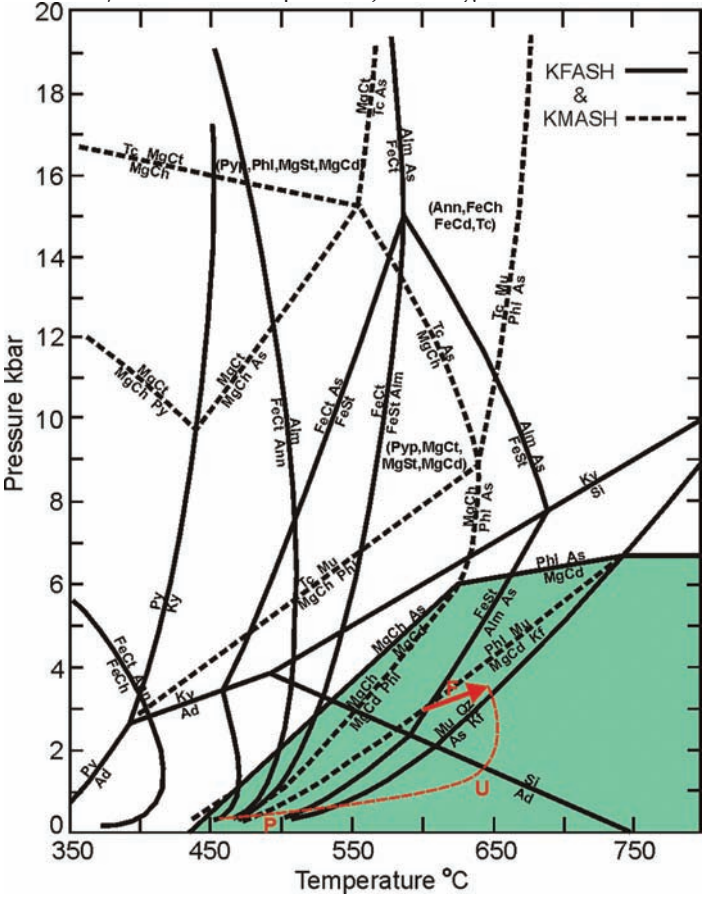

Fig. 5. *P-T diagram with essential mineral reactions of the KFASH (K_2O-FeO-Al_2O_3-SiO_2-H_2O) and the KMASH (K_2O-MgO-Al_2O_3-SiO_2-H_2O) system[2] as well as the approximate stability field of cordierite (green). The arrow indicates temperature and pressure during formation (F) of the ultramylonite, while the dashed curve represents respective P-T conditions during rock uplift (U) and pinitization (P). Abbreviations: Ad…andalusite, Alm…almandine, Ann…annite, As…alumosilicate, FeCd…Fe-cordierite, FeCh…Fe-chlorite, FeCt…Fe-chloritoid, FeSt…Fe-staurolite, Kf…K-feldspar, Ky…kyanite, MgCd…Mg-cordierite, MgCh…Mg-chlorite, MgCt…Mg-cloritoid, MgSt…Mg-staurolite, Mu…muscovite, Phl…phlogopite, Py…pyrophyllite, Pyp…pyrope, Qz…quartz, Si…sillimanite, Tc…talc.*

Side-By-Side Comparison? Difficult When Our Coaters Stand Alone.

High Resolution Sputter Coater 208HR for FE-SEM

Superior Features:

- High Resolution Fine Coating
- Wide Choice of Coating Materials
- High Resolution Thickness Control
- Multiple Sample Stage Movements
- Wide Range of Operating Pressures
- Compact, Modern, Benchtop Design

Find out about our complete line of sample coaters.

TED PELLA, INC.
Microscopy Products for Science and Industry

4595 Mountain Lakes Blvd., Redding, CA 96003-1448
Phone: 530-243-2200 or 800-237-3526 (USA) FAX: 530-243-3761
Email: sales@tedpella.com Web Site: www.tedpella.com

0.74 wt.% (Table 2). The sum of all octahedral cations ranges from 1.900 to 1.965, deviating from the ideal formula by 2 to 5 %. CaO and K_2O can be detected sometimes in very low amounts (0.002 to 0.009 wt.% and 0.001 to 0.002 wt.%, respectively), and therefore seem to be of negligible importance concerning the occupation of the crystal channels. In contrast, Na_2O is present in the channels with a concentration varying between 0.42 and 0.57 wt.%. The formulae listed in Table 2 yield evidence that the insertion of Na and K into the channels is mainly caused by a coupled substitution of (Na, K) + Al against the + Si channel site. The sum of all analyzed oxides ranges from 97.07 wt.% to 98.16 wt.% suggesting the introduction of about 2-3 wt.% of volatile compounds (H_2O, CO_2) into the crystal lattice (Table 2).

As could be established by several analyses on a single grain, cordierite from the ultramylonite does not show significant compositional zoning due to a possible variation of the $Mg/(Mg + Fe^{2+} + Mn)$ ratio from the crystal core to its rim. The ratio fluctuates between 0.561 and 0.566 (Table 2, analyses 5 and 6), but does not follow any remarkable trend. It must be noted that many cordierites of this micro-chemical investigation are characterized by a marginal replacement by pinite, which could be a reason for the destruction of a former compositional zoning.

Formation and decomposition (pinitization) of cordierite

Temperatures of mylonitization and cordierite formation were estimated using the Na-in-cordierite thermometer[11] and the garnet-cordierite Fe/Mg-exchange thermometer.[12] Temperatures calculated on the basis of the Na contents range from 586 to 630°C, exhibiting a significant decrease from the centre to the edge of the shear zone (Fig. 5). Garnet-cordierite temperatures, on the other hand, range from 593 to 639°C within a presumed pressure interval of 0.30–0.40 GPa, thereby showing a similar decrease along the shear zone profile as the temperatures derived from the Na-in-cordierite thermometer. Estimation of related pressures is mainly based on assumptions concerning the formation of cordierite and related mineral reactions, the stability of cordierite and its dependence on the Mg/(Mg + Fe) ratio, and the stability of other mineral constituents. A very coarse evaluation of pressure during metamorphism is possible by the fact that fibrolitic sillimanite is the only $AlSiO_5$ phase occurring in the studied mylonites. Considering a temperature range of 570–620°C and the stability field of sillimanite within the system kyanite–andalusite–sillimanite, pressure had to be higher than ca 0.35 GPa (Fig. 5).

The ultramylonite offers a possibility for studying various stages of cordierite decomposition during uplift of the host rock (Fig. 5). This so-called pinitization, which may be expressed by the chemical reaction

$$cordierite + biotite + H_2O \rightarrow muscovite + chlorite + quartz \quad (1)$$

and starts at temperatures of 475-500 °C[2], ranges from only poorly affected grains to fully transformed grains (Fig. 3a-f). In the first stage, cracks running through the mineral are continuously filled with very fine crystals of mica and chlorite (Fig. 3b-c). Subsequently, the margins of cordierite are transformed into muscovite, chlorite and biotite of variable size (Fig. 3c). In a medium stage of decomposition, internal pinitization undergoes a significant progression, forming aggregates of mainly mica, biotite, and chlorite (Fig. 3d). In the last stage of pinitization, the former cordierite has been fully transformed into bluish-green pinite which is demarcated from the matrix by a mantle of muscovite and biotite crystals. If the decomposition process is accomplished by local shear strain, the resulting pinitic blast is marked by a sigmoidal shape and internal microcrenulation (Fig. 3e-f).

When studied with the electron microprobe in back-scattered electron mode, pinites show a fine discontinuous corona of replacing minerals, which itself is surrounded by large grains of biotite and muscovite (Fig. 4). This outer corona demarcates the blast from the surrounding matrix, adjacent feldspar clasts, and relics of quartz.

Conclusion

As demonstrated by the study presented here, cordierite represents a metamorphic mineral phase of interest for the geoscientist but also for the microscopist. In petrographic thin-sections, the mineral is characterized by a typical appearance (see Fig. 3) and therefore can be easily distinguished from adjacent mineral phases with similar optical properties (*e.g.* quartz, untwinned feldspar). In micro-chemical respects, cordierite contains a significant amount of volatile phases (H_2O, CO_2) which may affect specific physical characteristics (*e.g.* colour, specific gravity, refraction index, *etc.*) to a certain degree. As exhibited by cordierite-rocks sampled from the South-western margin of the Bohemian Massif in Austria, cordierite is commonly formed during medium- to high-grade metamorphic deformation marked by temperatures > 500°C and lithological pressures < 0.6 GPa. During uplift and cooling of the lithological unit, within which cordierite was formed, the mineral phase is often subject to a typical decomposition process (see formula 1) that is widely known as pinitization. This process may also be of enhanced interest for microscopists, because within one rock sample, several stages of pinitization may be observed at the same time. Since factors controlling cordierite formation and decomposition are not fully decoded yet, the mineral will still be an object of increased geoscientific interest in future. ■

References

(1) Deer W. A., Howie, R. A. & Zussman J. (1992): An Introduction to the Rock-Forming Minerals. 2nd ed., Longmans Scientific and Technical, London.

(2) Spear, F. S. (1993): Metamorphic Phase Equilibria and Pressure-Temperature-Time Paths. Mineralogical Society of America (MSA), Washington D.C.

(3) Harker, A. (1939): Metamorphism. 2nd ed., Methuen & Co, London.

(4) Seifert, F. (1970): Low-temperature Compatibility Relations of Cordierite in Haplopelites of the System K2O—MgO—Al2O3—SiO2—H2O. Journal of Petrology 11, 73-100.

(5) Wall V. J., Clemens J. D. & Clarke, D. B. (1987): Models for granitoid evolution and source compositions. Journal of Geology 95, 731-750.

(6) Clarke, D. B. (1981): The mineralogy of peraluminous granites; a review. Canadian Mineralogist 19, 3-17.

(7) Clemens, J. D. & Wall, V. J. (1981): Origin and crystallization of some peraluminous (S-type) granitic magmas. Canadian Mineralogist 19, 111-131.

(8) Sturm, R. (2008): Microscopy and Microanalysis of Corona Textures in Eclogitic Greenschists from the Eastern Alps, Austria. Microscopy Today 16/2, 26-31.

(9) Kossmat, F. (1927): Gliederung des varistischen Gebirgsbaus. Abhandlungen der Sächsischen Geologischen Landesanstalt 1, 1-39.

(10) Frasl G. & Finger F. (1991): Geologisch-petrographische Exkursion in den österreichischen Teil des südböhmischen Batholiths. Beihefte zum European Journal of Mineralalogy 3, 23-40.

(11) Mirwald, P. W. (1986): Ist Cordierite in Geothermometer? Fortschritte der Mineralogie 64, 119.

(12) Perchuk, L. L. & Lavrent'eva, I. V. (1981): Experimental investigation of exchange equilibria in the system cordierite-garnet-biotite. In: Saxena, S. K. (ed.): Kinetics and Equilibrium in Mineral Reactions, Springer, New York, 199-240.

Would You Bet Your Company's Reputation on Your EDS Results? We Did.

NEW EXpert ID

We've Expanded Our Product Range with the Most Powerful SDD for EDS

- ***New*** **Apollo Silicon Drift Detector Enables Complete Spectrum Maps to be Collected in Seconds**
- ***New*** **Hikari High Speed EBSD Detector**
- **Seamless Integration of EDS, EBSD, and WDS**

The original expectations of the development of the Silicon Drift Detector are now achievable with the EDAX Apollo SDD. Fulfilling the promise of the new technology, the Apollo SDD is capable of collecting high count rates with excellent resolution in an LN_2 free environment. The Apollo SDD, when seamlessly integrated with the LambdaSpec WDS and the Hikari EBSD Detector, provides the ultimate in high speed analysis.

Results with Confidence...Even Faster

The Apollo SDD is the latest innovation from EDAX. As the world's leader in Electron Beam Microanalysis, EDAX continues to raise the performance standard with features that provide faster results that you can trust to be complete and accurate.

For more information on EDAX's latest product developments visit our web site at ***www.EDAX.com/NEW*** *or call* ***1-201-529-4880****.*

EDAX®
advanced microanalysis solutions

AMETEK®
MATERIALS ANALYSIS DIVISION